

# Attraction of spiral waves by localized inhomogeneities with small-world connections in excitable media

Xiaonan Wang, Ying Lu, Minxi Jiang, and Qi Ouyang\*

*Department of Physics, Peking University, Beijing 100871, People's Republic of China*

(Received 3 December 2003; published 27 May 2004)

Trapping and untrapping of spiral tips in a two-dimensional homogeneous excitable medium with local small-world connections are studied by numerical simulation. In a homogeneous medium which can be simulated with a lattice of regular neighborhood connections, the spiral wave is in the meandering regime. When changing the topology of a small region from regular connections to small-world connections, the tip of the spiral waves is attracted by the small-world region, where the average path length declines with the introduction of long distant connections. The “trapped” phenomenon also occurs in regular lattices where the diffusion coefficient of the small region is increased. The above results can be explained by the eikonal equation, the Luther equation, and the relation between the core radius and the diffusion coefficient.

DOI: 10.1103/PhysRevE.69.056223

PACS number(s): 82.40.Ck, 47.54.+r, 05.45.-a

## I. INTRODUCTION

Spiral waves are characteristic structures of excitable media that have been observed in many extended systems such as reaction-diffusion media [1–3], aggregating colonies of slime mold [4], and heart tissues [5], where they are suspected to play an essential role in cardiac arrhythmia and fibrillation. Sudden cardiac death resulting from ventricular fibrillation is generated from the fragmenting or breakup of spiral waves [6–8]. Spiral waves are prone to a variety of instabilities [9–11], one of which is meander instability [12,13], where spiral tips follow a hypocycloid trajectory instead of moving around a small circle. Due to the Doppler effect, this spiral may undergo a transition from ordered spiral patterns to a state of defect-mediated turbulence [11]. In the meandering regime, the spiral tips can be made to drift and can be controlled by external influences [14] or localized inhomogeneities of defects [15].

After the concept of small-world connections was proposed by Watts and Strogatz [16], it has quickly attracted much attention because this kind of connection exists commonly in real world, such as in social systems [17], neural networks [18], and epidemic problems [19]. Different studies show that a little change of the network connections can essentially change the features of a given medium, and plays a very important role in determining the dynamic behavior of a system.

In numerical simulations, a spatially extended system can be approximately regarded as a network consisting of a number of sites connected with certain topology. Thus localized inhomogeneities can be achieved by changing the topology of the network. In heart tissues, pacemakers dominate the dynamics of the traveling wave behavior and control the heart rhythm. We hypothesize that this happens because the characters and the structures of the local cells are different from other cardiac muscle cells. Could a small-world network describe one of the characters of the pacemaker? To

answer this question, we changed the widely used regular network in spiral wave study to a small-world network in part of the system to investigate its effects.

In the following section, we study the effect of a local small-world network on the behavior of spiral waves. We show that this special region is a dynamic attractor for spiral tips. In Sec. III, we compare the effect of the small-world network with that of the changing diffusion coefficient in the local region, and show that they are equivalent. We give a discussion and conclude our study in the last section.

## II. THE EFFECT OF SMALL-WORLD NETWORK

The model we used is the two-variable FitzHugh-Nagumo model [20] with local nearest-neighbor couplings in a region of  $N_1 \times N_2$ ,

$$\frac{du_{i,j}}{dt} = (a - u_{i,j})(u_{i,j} - 1)u_{i,j} - v_{i,j} + D_u \nabla^2 u_{i,j}, \quad (1)$$

$$\frac{dv_{i,j}}{dt} = \epsilon(bu_{i,j} - v_{i,j}) + D_v \nabla^2 v_{i,j}, \quad (2)$$

where  $i=1, 2, \dots, N_1, j=1, 2, \dots, N_2$ ;  $u_{i,j}(t)$  and  $v_{i,j}(t)$  are dimensionless excitable variable and recovery variable, respectively;  $D_u$  and  $D_v$  are diffusion coefficients of the two variables. The Laplacian in the last term can be approximated as

$$\nabla^2 u_{i,j} \cong \frac{1}{h^2}(u_{i-1,j} + u_{i+1,j} + u_{i,j-1} + u_{i,j+1} - 4u_{i,j}), \quad (3)$$

$$\nabla^2 v_{i,j} \cong \frac{1}{h^2}(v_{i-1,j} + v_{i+1,j} + v_{i,j-1} + v_{i,j+1} - 4v_{i,j}). \quad (4)$$

When  $0 < a < 1, b \geq 0, D_v \ll D_u, \epsilon \ll 1$ , the equation describes an excitable medium, which can be regarded as a simplified model for cardiac tissues. In the following discussion, we set the control parameters as follows:  $N_1 = N_2 = 256$  (space unit  $h=1$ ),  $a=0.1, b=1.0, \epsilon=0.005, D_u=0.33, D_v=0$ . No-flux boundary condition is applied in the simulation.

\*Electronic address: qi@pku.edu.cn

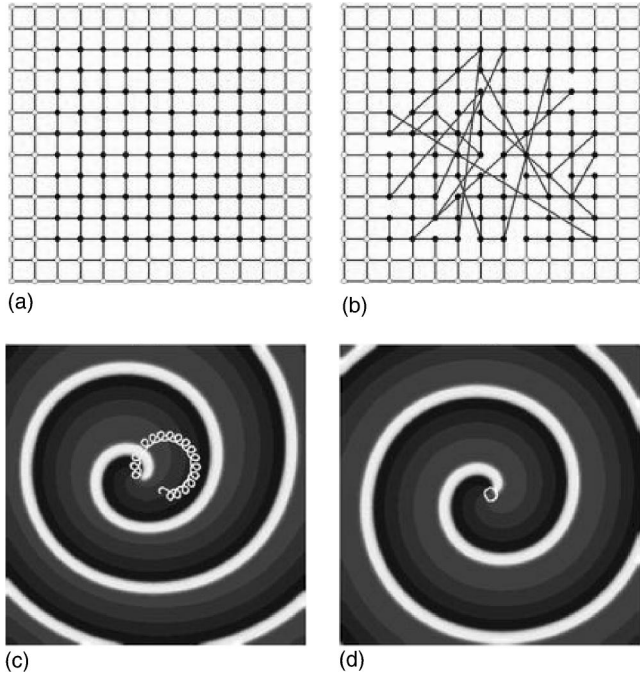


FIG. 1. Spiral pattern in different media. (a) a regular network,  $p_s=0$ ; (b) a small-world network,  $p_s=0.1$ ; (c) spiral wave and its tip's motion in the regular network. The white curve is the trajectory of the spiral tip; and (d) spiral wave and its tip's motion in the small-world network,  $N_s=10$ .

Using the vertical gradient distribution initial condition, we first create spiral waves in regular lattices [Fig. 1(a)]. In this case, the spiral tip follows a hypocycloid trajectory, showing a typical sign of meandering state [12], see Fig. 1(c). We then create a small-world network in a small local region  $\Omega$  of a size  $N_s N_s (N_s \ll N_1)$ , where the spiral tip locates. The small-world network is created in the following way: With the probability  $p_s (0 \leq p_s \leq 1)$ , we reconnect every edge in the region  $\Omega$  from one of its original vertex to another vertex chosen randomly in the region [16] [see Fig. 1(b)]. The change of connections leads to the change of “diffusion” mode. Supposing node  $[i][j]$  is connected with node  $[x_1][y_1]$ , node  $[x_2][y_2]$ , ... node  $[x_k][y_k]$ , then the diffusion term in the Eqs. (1) and (2) becomes

$$\nabla^2 u_{i,j} \cong \frac{1}{h^2} (u_{x_1,y_1} + u_{x_2,y_2} + \cdots + u_{x_k,y_k} - k u_{i,j}), \quad (5)$$

$$\nabla^2 v_{i,j} \cong \frac{1}{h^2} (v_{x_1,y_1} + v_{x_2,y_2} + \cdots + v_{x_k,y_k} - k v_{i,j}). \quad (6)$$

Introducing the small-world network region in the reaction medium greatly influences the motion of the spiral tip. We find that the small-world network region can attract the spiral tip as it passes through the region. After that the spiral tip rotates around its boundary, as shown in Fig. 1(d). Because the topological structure of the local small-world network is generated randomly under the rule mentioned above, the attraction only occurs with a certain probability under certain parameter range. To characterize the attraction prop-

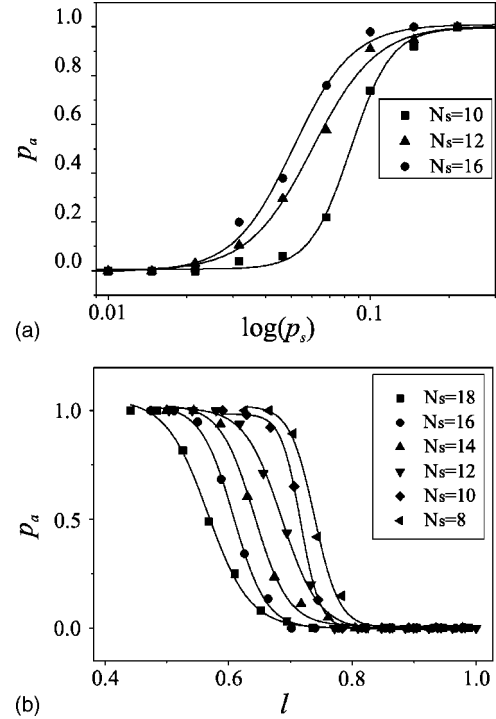


FIG. 2. (a) Transition curves of  $p_a$  as a function of  $p_s$  with different  $N_s$ . The solid lines are the sigmoidal fitting  $p_a=1/(1+\exp[(p_s-p_{sc})/dp_s])$ ; (b) transition curves of  $p_a$  as a function of  $l$  with different  $N_s$ . The solid lines are the fitting of  $p_a=1/(1+\exp[(l-l_c)/dl])$ . Here  $l_c$  is the critical length where  $p_a=0.5$ , and  $dl$  is the transition width.

erty of the small-world network, we use attraction probability  $p_a$  as an order parameter, which can be obtained by repeating (50 times in our work) the simulation using the same control parameters but with different small-world network connections. Our simulation results show that the most influential factor to  $p_a$  is the small-world creation probability  $p_s$ . As shown in Fig. 2(a),  $p_a$  increases with the increase of the small-world  $p_s$ . When  $p_s=0$  (corresponding to a regular network), the spiral tip cannot be attracted; when  $p_s=1$  the tip can be attracted with probability 1, which means the random network has a stronger attraction ability than the small-world network. Between  $0 < p_s < 1$ , there is a transition where the attraction probability  $p_a$  increases rapidly. The transition point  $p_c$  can be defined as the value of  $p_s$  when  $p_a=0.5$ .

One of the most important characters of small-world network is the reducing of the average path length while keeping the clustering coefficient  $C_v$  almost constant. The average path length is defined as the number of edges in the shortest path between two vertices, averaged over all pairs of vertices. The clustering coefficient is the average of  $C_v$  over all vector  $v$ .  $C_v$  denotes the ratio of the actually existing edges to the maximum allowable edges among all the neighbors of vector  $v$  [16]. Define the normalized average path length  $l$  of small-world network as  $l=L/L_0$ , where  $L$  is the average path length of small-world network in  $\Omega$  [21] and  $L_0$  is the average path length of regular network in  $\Omega$ .  $l$  will decrease from 1 to  $\varepsilon$  ( $\varepsilon > 0$ ) when  $p_s$  changes from 0 to 1. From our numerical simulations, we find the same type of

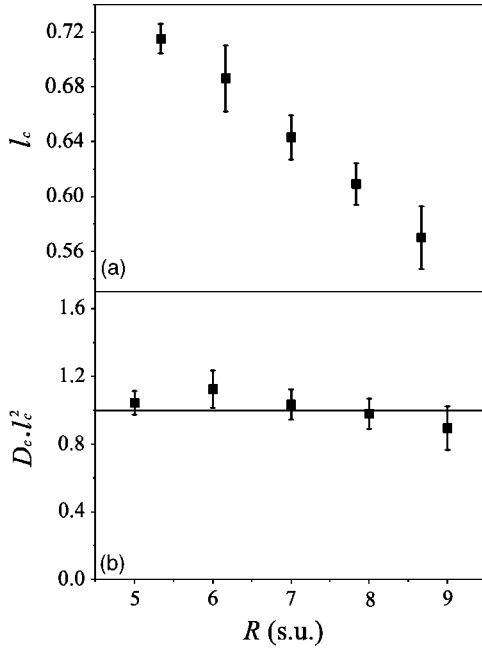


FIG. 3. (a) The critical length  $l_c$  as a function of the radius  $R$  of region  $\Omega$ , ( $R=Ns/2$ ), the error bar is  $dl$  [see the caption of Fig. 2(b) about the fitting]; (b)  $D_c l_c^2$  as a function of  $R$ .

transition curve of  $p_a$  as a function of  $l$ , as shown in Fig. 2(b), indicating that the major effect of the small-world topology to the behavior of spiral waves is the decrease of the average path length. In addition, defining the critical length  $l_c$  as the value of  $l$  when  $p_a=0.5$ , we find that the critical length decreases linearly with the increase of the size of  $\Omega$ , see Fig. 3(a).

### III. COMPARE WITH INCREASING THE DIFFUSION COEFFICIENT

Our simulation results suggest that the major effect of the small-world network on the spiral tip movement comes from the long-distance connections, which lead to shortening the average path length ( $l$ ) and increasing the diffusion speed. If the above suggestion is correct, the phenomenon of spiral tip attraction should also occur when we locally increase the diffusion constant in Eqs. (1) and (2). In this part of work, we increase the diffusion coefficient in a small circular region  $\Omega$  by  $D$  times and keep the system with regular connections. In the following discussion, we will use  $D_u^\Omega$  to denote the diffusion coefficient in region  $\Omega$ , and use  $D_u^0$  for the region outside of  $\Omega$ , so that  $D_u^\Omega = DD_u^0$ . We find that when  $D$  is large enough the spiral tip can be attracted by the region  $\Omega$  when it passes through it and then travels around it. At a given  $R$  ( $R > R_0$ ,  $R$  is the radius of  $\Omega$ ,  $R_0$  is the core radius of spiral when  $D_u^\Omega = D_u^0$ ), we can define two values  $D_1$  and  $D_2$ : A temporal attraction occurs when  $D_1 < D < D_2$ ; in this case the tip can be trapped for a short period and then escapes; the trapped time increases with  $D$ . When  $D > D_2$ , the tip can be trapped for a long enough period. Defining  $D_c$  as the mean value of  $D_1$  and  $D_2$ , the plot of  $D_c$  with different  $R$  is shown in Fig. 4.

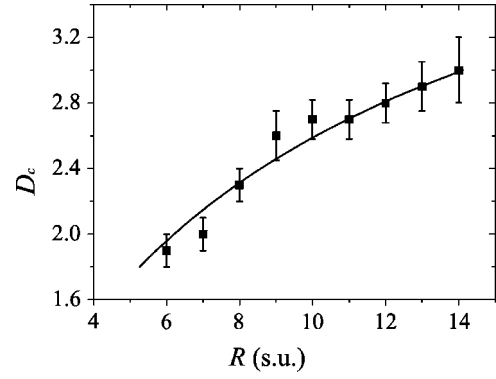


FIG. 4. The critical diffusion coefficient  $D_c$  as a function of  $R$ , where the line is the best fitting with Eq. (9). The error bars are estimated using  $D_1$  and  $D_2$ .

The above simulation results suggest that the increase of diffusion speed in the small region is responsible for the attraction of the spiral tip. To quantitatively compare the two systems, we analyze the diffusion terms of the two systems. In the small-world network, because of the long-distance connections, the average distance between nodes declines as  $p_s$  increases from 0 to 1. In a network model of a reaction-diffusion system, this effect can be in a sense translated from the decrease of the average path length between nodes while keeping the distance of two neighboring nodes  $h$  constant, to the decrease of the step length  $h$  while keeping the network regular. The normalized average path length  $l$  can also describes the relative change of  $h$ . From this argument, the diffusion items of the small-world network can be expressed as

$$D_u^0 \frac{1}{(lh)^2} (u_{i-1,j} + u_{i+1,j} + u_{i,j-1} + u_{i,j+1} - 4u_{i,j}), \quad (7)$$

$$D_v^0 \frac{1}{(lh)^2} (v_{i-1,j} + v_{i+1,j} + v_{i,j-1} + v_{i,j+1} - 4v_{i,j}). \quad (8)$$

At the critical point, for a fixed  $R$ , the diffusion terms in two systems should be the same. So that  $D_u^\Omega 1/h^2 = D_c D_u^0 1/h^2 = D_u^0 1/(l_c h)^2$ , which gives  $D_c l_c^2 = 1$ . As presented in Fig. 3(b), our simulation fits this analysis within the range of error. This result indicates that our proposition is reasonable. The attracting effect of the small-world network comes from the decline of  $l$  inside the inhomogeneous area  $\Omega$ .

### IV. DISCUSSION

A question should be answered before fully understanding the effect of the small-world network in the dynamics of spiral tips: what is the mechanism for the spiral tip attraction? In the following discussion, we give an explanation with eikonal equation, Luther equation [22], and the relation between the diffusion coefficient and the spiral core radius. According to the analysis of the spiral tip dynamics given by Hakim and Karma [23], for the steady rotational movement of a spiral tip in an excitable medium, the core radius  $R$  as a function of diffusion coefficient can be written as

$$R = \frac{D_u}{c_0} \left( \frac{bK}{B_c - \frac{2D_u}{W}} \right)^{3/2}, \quad (9)$$

where  $D_u$  is the diffusion coefficient of the activator ( $u$ );  $c_0$  is the speed of plane wave;  $b$ ,  $K$ , and  $B_c$  are all constants.  $W$  is the constant width of the excited region. In the simulation, we assume that at the boundary of  $\Omega$  there exists a “virtual” gradient region of  $D_u$  which links the outside and inside regions. For a given  $R$  of the region  $\Omega$  [ $R > R_0 = R(D_u^0)$ ], the “trapped” motion of the spiral tip requires a specific value of  $D_u$ , satisfying Eq. (9). When  $D_u < D_u^0$ , the spiral tip will enter the gradient region where the system can find the required  $D_u$ , so that the spiral tip will rotate around the gradient area at the boundary of  $\Omega$ ; on the other hand, when  $D_u > D_u^0$ , the trapped motion cannot be sustained by the central region. From this argument, at critical point, we will have  $D_u(R) = D_u^0 = D_c D_u^0$ . As shown in Fig. 4, our simulation results are consistent with this analysis within the range of error.

To prove the trapped state of spiral tip motion is a stable state, we apply the eikonal equation, which determines the relation between the curvature of a traveling wave front and its speed in an excitable medium, and the Luther relation, which describes the relation between the speed of chemical waves and the diffusion coefficient of activator [22]. The eikonal equation is  $N = C - D_u \kappa$ , where  $N$  is the normal wave speed,  $\kappa$  is the local curvature of the wave front; the Luther equation is:  $c = \alpha \sqrt{D_u}$ , where  $\alpha$  is a constant. Insert the Luther equation into the eikonal relation we have

$$N = \alpha \sqrt{D_u} - D_u \kappa. \quad (10)$$

Taking partial derivative of  $R$  in Eq. (10), we get

$$\frac{\partial N}{\partial R} = \left[ \frac{1}{2} \alpha (D_u)^{-1/2} - \kappa \right] \frac{\partial D_u}{\partial R}. \quad (11)$$

At the spiral tip we have  $N=0$ , so that

$$\frac{\partial N}{\partial R} \Big|_{\text{tip}} = -\frac{1}{2} \kappa_{\text{tip}} \frac{\partial D_u}{\partial R}. \quad (12)$$

In our system, assuming a continuous change of  $D_u$  at the boundary of region  $\Omega$ , we have  $\partial D_u / \partial R < 0$ . Thus Eq. (12) indicates that  $(\partial N / \partial R)|_{\text{tip}} > 0$ . That means, if we introduce a small deviation from the trapped motion of the spiral tip, the system will return to the trapped state spontaneously, because we have  $N < 0$  inside the region  $\Omega$ , and  $N > 0$  outside the region  $\Omega$  ( $\hat{n}$  points to the center of  $\Omega$  region).

In conclusion, we find that in an excitable system local change of topological structure can trap the spiral tip. This ability comes from the increase of diffusion speed. We prove this by increasing the diffusion coefficient. We also give a theoretical explanation using eikonal equation, Luther equation, and the relation between the core radius and the diffusion coefficient, which fits well with the results of simulation. We should note that there are other situations where the tip of spiral waves can be trapped in a given area. For example, Lázár *et al.* reported that self-sustained chemical waves can rotate around a central obstacle in an annular two-dimensional excitable system, and the wave fronts in the case of an annular excitable region are purely involutes of the central obstacle in the asymptotic state [24]. Obviously this phenomenon is beyond our analysis. More work should be done to fully understand the attractive effect of local inhomogeneities in an excitable reaction-diffusion system.

## ACKNOWLEDGMENTS

This work was partly supported by the grants from Chinese Natural Science Foundation, Department of Science of Technology in China and financial support from Peking University.

- 
- [1] A. N. Zakin and A. M. Zhabotinsky, *Nature (London)* **225**, 535 (1970).  
 [2] L. Q. Zhou and Q. Ouyang, *Phys. Rev. Lett.* **85**, 1650 (2000).  
 [3] L. Q. Zhou and Q. Ouyang, *J. Phys. Chem. A* **105**, 112 (2001).  
 [4] K. J. Lee, E. C. Cox, and R. E. Goldstein, *Phys. Rev. Lett.* **76**, 1174 (1996).  
 [5] J. M. Davidenko, A. M. Pertsov, R. Salomonz, W. Baxter, and J. Jalife, *Nature (London)* **335**, 349 (1992).  
 [6] J. N. Weiss, A. Garfinkel, H. S. Karagueuzian, and P. S. Chen, *Circulation* **99**, 2819 (1999).  
 [7] M. L. Riccio, M. L. Koller, and R. F. Gilmour, *Circ. Res.* **84**, 955 (1999).  
 [8] L. Glass, *Phys. Today* **8**, 40 (1996).  
 [9] Q. Ouyang and J.-M. Flesselles, *Nature (London)* **379**, 143 (1996).  
 [10] A. Belmonte, J.-M. Flesselles, and Q. Ouyang, *Europhys. Lett.* **35**, 665 (1996).  
 [11] Q. Ouyang, H. L. Swinney, and G. Li, *Phys. Rev. Lett.* **84**, 1047 (2000).  
 [12] G. Li, Q. Ouyang, V. Petrov, and H. L. Swinney, *Phys. Rev. Lett.* **77**, 2105 (1996).  
 [13] D. Barkley, *Phys. Rev. Lett.* **68**, 2090 (1992).  
 [14] K. I. Agladze and P. DeKepper, *J. Phys. Chem.* **96**, 5239 (1992).  
 [15] S. Nettesheim, A. von Oertzen, H. H. Rotermund, and G. Ertl, *J. Chem. Phys.* **98**, 9977 (1993).  
 [16] D. J. Watts and S. H. Strogatz, *Nature (London)* **393**, 440 (1998).  
 [17] J. J. Collins and C. C. Chow, *Nature (London)* **393**, 409 (1998).  
 [18] J. J. Hopfield and A. V. M. Herz, *Proc. Natl. Acad. Sci. U.S.A.* **92**, 6655 (1995).

- [19] S. A. Pandit and R. E. Amritkar, Phys. Rev. E **60**, R1119 (1999).
- [20] R. A. FitzHugh, Biophys. J. **1**, 445 (1966).
- [21] R. Albert and A. L. Barabasi, Rev. Mod. Phys. **74**, 47 (2002).
- [22] R. Arnold, K. Showalter, and J. J. Tyson, J. Chem. Educ. **64**, 740 (1987).
- [23] V. Hakim and A. Karma, Phys. Rev. E **60**, 5073 (1999).
- [24] A. Lázár, Z. Nosztizius, and H. Farkas, Chaos **2**, 443 (1995).